

# Finite-difference Modeling of EM Fields Using Coupled Potentials in 3D Anisotropic Media: Application to Borehole Logging

Junsheng Hou\* and Carlos Torres-Verdin, The University of Texas at Austin, USA

## Summary

We present a staggered finite-difference (FD) forward modeling algorithm of computing frequency-domain EM fields using coupled potentials in 3D inhomogeneous anisotropic media. This algorithm is based on the partial differential equations (PDE) for coupled vector and scalar potentials subject to the appropriate boundary conditions, which are approximated using central FD on a Yee's staggered grid. After discretization, a complex matrix equation is assembled, and is iteratively solved using complex bi-conjugate gradient method with preconditioning such as SSOR and Jacobi preconditioners. For the homogeneous full space, 1D and 2D layered anisotropic formations, we compared the numerical results from our algorithm with analytical solutions, our own 2D coupled potential FD solutions and 3D direct field FD solutions, and found excellent agreements between them. We also discussed the influences on iterative convergence rate using different frequencies and conductivity contrasts. To illustrate practical applications of this new algorithm, we conducted some more complicated model simulations. All numerical examples show that the algorithm can efficiently simulate EM fields in 3D inhomogeneous anisotropic media with highly discontinuous anisotropic conductivities over a wide range of frequencies.

## Introduction

Some various EM finite-difference (FD) numerical simulations have been extensively applied to 3D EM geophysics in the recent years (for example, Smith, 1996; LaBrecque, 1999; Haber et al, 2001; Wang et al, 2001, and Hou et al, 2002). These numerical simulation approaches may be based on directly solving Maxwell's equations, or the second order partial differential equations (PDE) governing electric or magnetic fields, called direct field methods, or the second order PDEs governing potentials, called potential methods. Potential methods are now becoming more prevalent for FD modeling in the EM domain, especially at low frequencies. For example, Smith (1996) developed a corrected algorithm for the direct field method using scalar potential. LaBrecque (1999) derived the coupled potential formulations using the standard-grid FD in isotropic media. Druskin et al (1999), Haber et al (2001), and Newman et al (2002) used the different potential formulations from LaBrecque (1999) for EM modeling in isotropic media. Chin (1999, personal communication) presented a coupled potential method using the standard grid FD in block-constant transversely isotropic media. Based on past research, these potential formulations have some advantages compared to the direct field modeling.

For example, they can overcome the problems of spurious modes resulting from using the "curl-curl" equation of direct fields at low frequencies. Hence, these potential formulations are able to calculate results over a very broad frequency range. Since the potentials are continuous everywhere, they can handle large conductivity contrasts.

According to the advantages of the potential formulations, following LaBrecque (1999) we will conduct FD modeling of EM fields at a staggered grid using the 2nd-order coupled (vector-scalar) potential PDEs in 3D inhomogeneous anisotropic media for borehole EM logging.

## Theory

Assuming a time harmonic dependence of  $e^{i\omega t}$ , in frequency domain Maxwell's equations can be expressed as (SI unit)

$$\begin{aligned} \hat{\mathbf{1}} \tilde{\mathbf{N}} \cdot \mathbf{E} &= -i\omega \mathbf{m}_0 \mathbf{H} \\ \hat{\mathbf{1}} \tilde{\mathbf{N}} \cdot \mathbf{H} &= \mathbf{s} \cdot \mathbf{E} + \mathbf{J}_p \end{aligned} \quad (1)$$

Here  $\mathbf{E}$  and  $\mathbf{H}$  are the electric and magnetic field vectors, respectively;  $\mathbf{J}_p$  is the current density vector of the external

electric current source;  $\mathbf{s}' = \mathbf{s} + i\omega \mathbf{e}$  is the complex conductivity,  $\mathbf{s}$  is the conductivity, and  $\mathbf{e}$  is the dielectric permittivity, and  $\mathbf{m}_0$  is the free space magnetic permeability;

$i = \sqrt{-1}$ , and  $\omega$  is the angular frequency. From Maxwell's equations (1), we can get the following coupled PDEs governing the vector-scalar potentials

$$\tilde{\mathbf{N}}^2 \mathbf{A} - i\omega \mathbf{m}_0 \mathbf{s}' \cdot \mathbf{A} - \mathbf{m}_0 \mathbf{s}' \times \tilde{\mathbf{N}} \mathbf{V} = -\mathbf{m}_0 \mathbf{J}_p \quad (2)$$

$$\tilde{\mathbf{N}} \cdot (\mathbf{s}' \times \tilde{\mathbf{N}} \mathbf{V}) + i\omega \tilde{\mathbf{N}} \cdot (\mathbf{s}' \cdot \mathbf{A}) = \tilde{\mathbf{N}} \cdot \mathbf{J}_p \quad (3)$$

Here  $\mathbf{A}$  is called the vector potential and satisfies the Coulomb gauge, and  $V$  is called the scalar potential. This system is defined over an unbounded spatial domain  $\Omega = R^3$ , but, in practice, a bounded sub-domain of  $\Omega$  will be used for our real numerical simulation. In order to complete the specification of this system, in our research the homogeneous Dirichlet and mixed boundary conditions for coupled potentials have been used. Hence, the EM forward modeling reduces to solving the boundary-value problem consisting of equations (2) and (3) subject to the boundary conditions. We also know that there are the relationships between EM fields and coupled potentials, namely  $\mathbf{E} = -i\omega \mathbf{A} - \nabla V$ ,  $\mathbf{J} = \mathbf{s}' \cdot \mathbf{E}$  and  $\mathbf{H} = (1/\mathbf{m}_0) \tilde{\mathbf{N}} \cdot \mathbf{A}$ . It is evident that if the scalar and

## EM modeling using potentials

vector potentials are known, the EM fields may be calculated directly from these equations.

For example, if we assume the complex conductivity  $\mathbf{S}'$  is a symmetric and non-negative  $3 \times 3$  tensor, and it can be

$$\text{expressed as } \mathbf{S}' = \mathbf{S}'(x, y, z) = \begin{pmatrix} \mathbf{s}'_{xx} & \mathbf{s}'_{xy} & \mathbf{s}'_{xz} \\ \mathbf{s}'_{yx} & \mathbf{s}'_{yy} & \mathbf{s}'_{yz} \\ \mathbf{s}'_{zx} & \mathbf{s}'_{zy} & \mathbf{s}'_{zz} \end{pmatrix}, \text{ we}$$

rewrite the coupled PDEs (2) and (3) in terms of components, and obtain in the rectangular coordinate system

$$\begin{aligned} & \tilde{N}^2 A_x - i\omega \mathbf{m}_0 (\mathbf{s}'_{xx} \times A_x + \mathbf{s}'_{xy} \times A_y + \mathbf{s}'_{xz} \times A_z) \\ & - \mathbf{m}_0 (\mathbf{s}'_{xx} \times \frac{\partial V}{\partial x} + \mathbf{s}'_{xy} \times \frac{\partial V}{\partial y} + \mathbf{s}'_{xz} \times \frac{\partial V}{\partial z}) = -\mathbf{m}_0 J_{px} \\ & \tilde{N}^2 A_y - i\omega \mathbf{m}_0 (\mathbf{s}'_{yx} \times A_x + \mathbf{s}'_{yy} \times A_y + \mathbf{s}'_{yz} \times A_z) \\ & - \mathbf{m}_0 (\mathbf{s}'_{yx} \times \frac{\partial V}{\partial x} + \mathbf{s}'_{yy} \times \frac{\partial V}{\partial y} + \mathbf{s}'_{yz} \times \frac{\partial V}{\partial z}) = -\mathbf{m}_0 J_{py} \\ & \tilde{N}^2 A_z - i\omega \mathbf{m}_0 (\mathbf{s}'_{zx} \times A_x + \mathbf{s}'_{zy} \times A_y + \mathbf{s}'_{zz} \times A_z) \\ & - \mathbf{m}_0 (\mathbf{s}'_{zx} \times \frac{\partial V}{\partial x} + \mathbf{s}'_{zy} \times \frac{\partial V}{\partial y} + \mathbf{s}'_{zz} \times \frac{\partial V}{\partial z}) = -\mathbf{m}_0 J_{pz} \\ & \frac{\partial}{\partial x} (P_x \frac{\partial V}{\partial x}) + \frac{\partial}{\partial y} (P_y \frac{\partial V}{\partial y}) + \frac{\partial}{\partial z} (P_z \frac{\partial V}{\partial z}) + \\ & i\omega \frac{\partial P_x}{\partial x} A_x + i\omega \frac{\partial P_y}{\partial y} A_y + i\omega \frac{\partial P_z}{\partial z} A_z \\ & + i\omega (P_x - P_y) \frac{\partial A_x}{\partial x} + i\omega (P_z - P_y) \frac{\partial A_z}{\partial z} = \tilde{N} \cdot \mathbf{J}_p \end{aligned}$$

Where  $P_x = \mathbf{s}'_{xx} + \mathbf{s}'_{yx} + \mathbf{s}'_{zx}$ ;  $P_y = \mathbf{s}'_{xy} + \mathbf{s}'_{yy} + \mathbf{s}'_{zy}$ ;

$P_z = \mathbf{s}'_{xz} + \mathbf{s}'_{yz} + \mathbf{s}'_{zz}$ ;  $\mathbf{J}_p = J_{px} \mathbf{i} + J_{py} \mathbf{j} + J_{pz} \mathbf{k}$ ;

and  $A_x, A_y, A_z$  are three components of the vector potential in x, y and z directions. Next we will solve these PDEs using the staggered FD method.

To solve the 3D boundary-value problem of coupled potentials by the FD method, we divide the solution domain into  $(N_x N_y N_z)$  rectangular cells in the rectangular coordinate system. We employ central FD approximation on the Yee's staggered grid (Yee, 1966), where  $\mathbf{A}$  is located at the center of the edges of the cell, and  $V$  is located at the corner of the cell. We write the fully discretized boundary-value problem as

$$F X = B \quad (4)$$

Or

$$\begin{pmatrix} \mathbf{a} & \mathbf{0} & \mathbf{0} & \mathbf{0} \\ \mathbf{c} & \mathbf{T}^1 & \mathbf{T}^2 & \mathbf{T}^3 \\ \mathbf{c} & \mathbf{U}^1 & \mathbf{U}^2 & \mathbf{U}^3 \\ \mathbf{c} & \mathbf{W}^1 & \mathbf{W}^2 & \mathbf{W}^3 \end{pmatrix} \begin{pmatrix} \mathbf{A}_x \\ \mathbf{A}_y \\ \mathbf{A}_z \\ \mathbf{V} \end{pmatrix} = \begin{pmatrix} \mathbf{b}_x \\ \mathbf{b}_y \\ \mathbf{b}_z \\ \mathbf{b}_v \end{pmatrix}$$

Here  $F = (a_{ij})_{N \times N}$  is the coefficient matrix of the matrix equation, it is a non-symmetric complex matrix, and there are only limited nonzero elements in a row of the matrix. Hence  $F$  is a large, sparse, and band matrix; its elements mainly depend on the grid spacing and medium conductivity;  $N = m_1 + m_2 + m_3 + m_4$ ,

$$m_1 = N_x \cdot (N_y - 1) \cdot (N_z - 1),$$

$$m_2 = (N_x - 1) \cdot N_y \cdot (N_z - 1),$$

$$m_3 = (N_x - 1) \cdot (N_y - 1) \cdot N_z,$$

$$m_4 = (N_x - 1) \cdot (N_y - 1) \cdot (N_z - 1);$$

$X$  is the unknown vector of complex values of the potentials throughout the model;  $B$  is the right-hand vector containing source terms associated with the boundary conditions.

$$X = (A_x, A_y, A_z, V)^T, B = (b_x, b_y, b_z, b_v)^T,$$

$$S^1 = (S^1_{i_1 j_1})_{m_1 \times m_1}, S^2 = (S^2_{i_2 j_2})_{m_2 \times m_2}$$

$$S^3 = (S^3_{i_3 j_3})_{m_3 \times m_3}, S^4 = (S^4_{i_4 j_4})_{m_4 \times m_4}, T^1 = (T^1_{i_2 j_1})_{m_2 \times m_1},$$

$$T^2 = (T^2_{i_2 j_2})_{m_2 \times m_2}, T^3 = (T^3_{i_2 j_3})_{m_2 \times m_3}, T^4 = (T^4_{i_2 j_4})_{m_2 \times m_4},$$

$$U^1 = (U^1_{i_3 j_1})_{m_3 \times m_1}, U^2 = (U^2_{i_3 j_2})_{m_3 \times m_2},$$

$$U^3 = (U^3_{i_3 j_3})_{m_3 \times m_3}, U^4 = (U^4_{i_3 j_4})_{m_3 \times m_4},$$

$$W^1 = (W^1_{i_4 j_1})_{m_4 \times m_1}, W^2 = (W^2_{i_4 j_2})_{m_4 \times m_2},$$

$$W^3 = (W^3_{i_4 j_3})_{m_4 \times m_3}, W^4 = (W^4_{i_4 j_4})_{m_4 \times m_4}.$$

Hence, the EM forward modeling is equivalent to solving the discretized linear system (4). Since the linear system (4) is a non-symmetric complex linear one, we solve it using the complex bi-conjugate gradient algorithm (CBCG). To accelerate its rate of convergence, we precondition the linear system before we solve it. Therefore, we call the overall scheme the preconditioned complex bi-conjugate gradient algorithm or PCBCG. We have used the preconditioning methods in our numerical simulation; for example, Jacobi, ILU, and SSOR preconditioners (Axelsson, 1994).

### Numerical examples

We have implemented the algorithm, and in this section we will present some numerical examples of borehole EM

## EM modeling using potentials

modeling by using our code for solving the resulting discrete systems. In the following numerical experiments, a  $40 \times 40 \times 40$  variable grid and an electrical dipole source located at  $z=0$  (the borehole axis) with moment  $10 \text{ A} \cdot \text{m}$  are used. The background conductivity is  $\sigma_b = 0.2 \text{ s/m}$ . The formation is a layer with a thickness 6m and its invasion zone's radius is 1m, the invasion conductivity is  $1 \text{ s/m}$  and  $2 \text{ s/m}$ . The formation anisotropic factor of conductivity is 2.

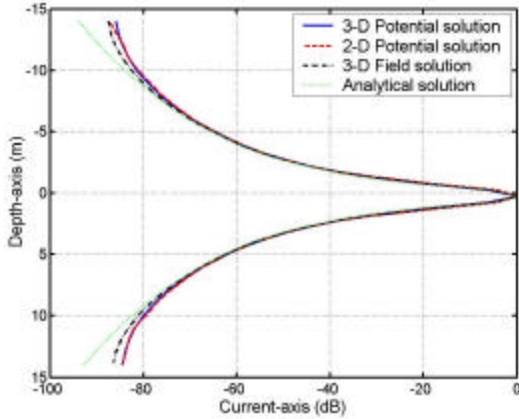


Fig. 1: Borehole currents in the homogeneous full space

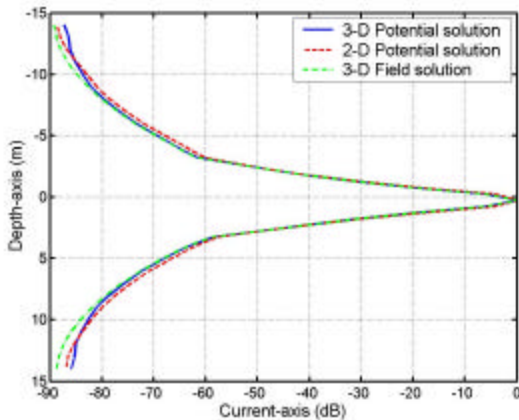


Fig. 2: Borehole currents in 2D anisotropic layered formation

### (1) Code validation

In order to check this code some numerical tests are conducted. Let EM frequency be 10kHz. Checks that are made include: (1) checks against the analytical solution to the full space; (2) comparison with the solutions from our 2D potential and 3D direct field programs using 1D layered formation and 2D models (1D with invasion); (3) consistency of the solutions with conservation laws that must hold at all frequencies. Some results are shown in Figure 1-2. All of them show the excellent agreements of the solutions between this code and the analytical, our 2D potential and 3D field solutions. From

Figure 2, we also find the vertical current is continuous across the formation interface, so the conservation law is held.

### (2) Effect of different frequencies and conductivity contrasts

Next, we demonstrate the effect of using different frequencies on iterative convergence. The numerical results are summarized in Table 1-2. They show that the iterative convergence is insensitive to the change of frequencies less than 1kHz. We also test the effect of using different conductivity contrasts on iterative convergence. They are gathered in Table 3-4. It is easy to note that large jump conductivity contrast ( $10^{-6}$  to  $10^6$ ) do not significantly affect the rate of convergence of our equation solvers.

### (3) Application to 3D models

The application to a 3D anisotropic model is shown in Fig.3-4.

## Conclusions

In this paper, we have developed and implemented a fast staggered FD modeling algorithm using coupled potentials for the solution of Maxwell's equations of frequency domain in a 3D anisotropic medium with large conductivity contrasts at low to high frequencies (for example, 0-1MHz) on a personal computer. The resulting algorithm was tested on a variety of EM forward problems.

## References

- Axelsson, O., 1994, Iterative solution methods: Cambridge University Press.
- Druskin, V., Knizhnerman, L., and Lee, P., 1999, New spectral Lanczos decomposition method for induction modeling in arbitrary 3D geometry: *Geophysics*, **64**, 701-706.
- Haber, E. and Ascher, U. M., 2001, Fast finite volume simulation of 3D electromagnetic problems with highly discontinuous coefficients: *SIAM J. SCI. COMPUT.*, **22**, 1943-1961.
- Hou, J. and Torres-Verdin, C., 2002, Progress report on the development of a finite-difference FORTRAN code for the numerical simulation of EM phenomena in 3D anisotropic formations-applications to induction logging: Presented at the second formation evaluation annual conference, UT at Austin.
- LaBrecque, D. J., 1999, Finite difference modeling of 3-D EM fields with scalar and vector potentials, in Oritaglio, M., and Spies, B., Eds., *Three-dimensional electromagnetics: Soc. Expl. Geophys*, 146-160.
- Newman, G. A., and Alumbaugh, D.L., 2002, Three-dimensional induction logging problems, Part 2: A finite difference solution, *Geophysics*: **67**, 484-491.
- Smith, J. T., 1996, Conservative modeling of 3-D electromagnetic fields, Part I: Properties and error analysis: *Geophysics*, **61**, 1308-1318.
- Wang, T. and Fang, S., 2001, 3-D electromagnetic anisotropy

## EM modeling using potentials

modeling using finite differences: Geophysics, **66**, 1386-1398.  
 Yee, K.S., 1966, Numerical solution of initial boundary value problems involving Maxwell's equations in isotropic media: IEEE Trans. Antennas Prop., **AP-14**, 302-307.

Table 1. Iterative convergent results of 1D layered anisotropic formation using different frequencies

Frequency (Hz)	Iterative number	Iterative error ( $\times 10^{-8}$ )
0	19	0.7850
1	22	0.4188
10	22	0.7051
$10^2$	24	0.9625
$10^3$	27	0.4322
$10^4$	29	0.7325
$10^5$	37	0.2623
$10^6$	80	0.8752

Table 2. Iterative convergent results of 3D layered anisotropic formation using different frequencies

Frequency (Hz)	Iterative number	Iterative error ( $\times 10^{-8}$ )
0	20	0.5220
1	24	0.7732
10	27	0.6866
$10^2$	27	0.9464
$10^3$	35	0.5555
$10^4$	37	0.7402
$10^5$	41	0.9546
$10^6$	95	7.0496

Table 3. Iterative convergent results for different conductivity contrasts of 3D anisotropic media when layered formation conductivity  $S_f$  is increased

$S_f / S_b$	Iterative number	Iterative error ( $\times 10^{-8}$ )	Remarks
1	23	0.9818	$S_b = 0.2 \text{ s/m}$ Frequency=5Hz
10	19	0.9296	
$10^2$	14	0.8716	
$10^3$	13	0.6466	
$10^4$	13	0.6393	
$10^5$	19	9.0883	
$10^6$	21	3.3674	

Table 4. Iterative convergent results when  $S_f$  is decreased

$S_f / S_b$	Iterative number	Iterative error ( $\times 10^{-8}$ )	Remarks
1	23	0.9818	$S_b = 0.2 \text{ s/m}$ Frequency=5Hz
$10^{-1}$	21	7.5014	
$10^{-2}$	21	9.5374	
$10^{-3}$	21	9.5519	
$10^{-4}$	21	9.5048	
$10^{-5}$	21	9.5397	
$10^{-6}$	21	9.5396	

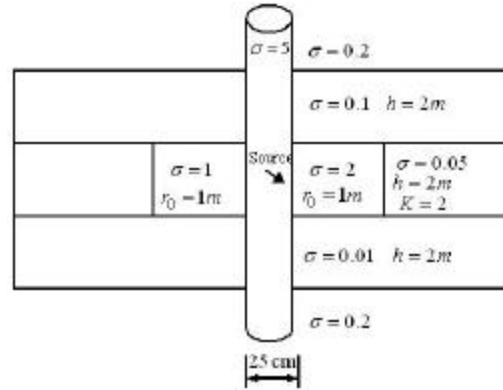


Fig. 3: 3D anisotropic formation. The applied parameters are as shown,  $S$  is the conductivity (s/m),  $h$  is the formation thickness,  $r_0$  is the radius of the invaded zone,  $K$  is the anisotropic factor, and the source is a dipping electric dipole.

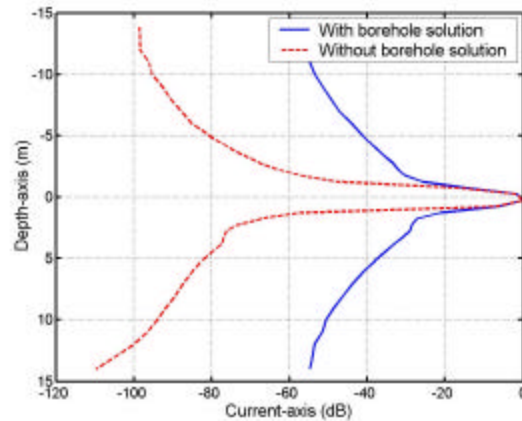


Fig. 4: Borehole vertical currents with and without borehole effects in a 3D anisotropic layered formation